J Membrane Biol (2007) 215:169–180
DOI 10.1007/s00232-007-9016-1

Accessibility of Four Arginine Residues on the S4 Segment of the *Bacillus halodurans* Sodium Channel

Jonathan Blanchet · Mohamed Chahine

Received: 12 December 2006 / Accepted: 28 February 2007 / Published online: 14 June 2007

Abstract The voltage-gated Na^+ channel of *Bacillus halodurans* (NaChBac) is composed of six transmembrane segments (S1–S6), with a pore-forming region composed of segments S5 and S6 and a voltage-sensing domain composed of segments S1–S4. The S4 segment forms the core of the voltage sensor. We explored the accessibility of four arginine residues on the S4 segment of NaChBac, which are positioned at every third position from each other. These arginine residues on the S4 segment were replaced with cysteines using site-directed mutagenesis. Na^+ currents were recorded using the whole-cell configuration of the patch-clamp technique. We tested the effect of the sulfhydryl reagents applied from inside and outside the cellular space in the open and closed conformations. Structural models of the voltage sensor of NaChBac were constructed based on the recently crystallized KvAP and Kv1.2 K^+ channels to visualize arginine residue accessibility. Our results suggest that arginine accessibility did not change significantly between the open and closed conformations, supporting the idea of a small movement of the S4 segment during gating. Molecular modeling of the closed conformation also supported a small movement of S4, which is mainly characterized by a rotation and a tilt along the periphery of the pore. Interestingly, the second arginine residue of the S4 segment (R114) was accessible to sulfhydryl reagents from both sides of the membrane in the closed conformation and, based on our model, seemed to be at the junction of the intracellular and extracellular water crevices.

Keywords Voltage-gated Na^+ channel · Gating charge · S4 segment · Voltage sensor · *Bacillus halodurans* · NaChBac · Methanethiosulfonate · 2-(Trimethylammonium)ethyl]-methanethiosulfonate

Introduction

Voltage-gated Na^+ channels are transmembrane proteins that control the movement of Na^+ ions of many excitable cells (Hille, 2001; Armstrong & Hille, 1998). NaChBac, a prokaryotic voltage-gated Na^+ channel from *Bacillus halodurans* (Ren et al., 2001), has recently been cloned and is a very attractive model for studying the structure and function of voltage-gated ion channels. A detailed study of the biophysical properties of NaChBac is warranted because of its potential for crystallization. It is composed of six transmembrane segments (S1–S6), with a voltage-sensing domain formed by S1–S4 (where S4 plays a central role in voltage sensing) and an atypical pore region flanked by the S5 and S6 transmembrane segments (Ren et al., 2001; Chahine et al., 2004). While this channel is Na^+-selective, the amino acid sequence of the selectivity filter is more homologous to calcium channels, in particular because of the presence of a conserved glutamate residue that is known to play an important role in Ca^{2+} selectivity.

The recent crystallization of the KvAP and Kv1.2 channels has provided useful insights into channel structure

J. Blanchet · M. Chahine
Department of Medicine, Le Centre de recherche Université Laval Robert-Giffard, Québec, QC, Canada G1J 2G3

M. Chahine (✉)
Le Centre de recherche Université Laval Robert-Giffard, 2601 chemin de la Canardière, Québec, QC, Canada G1J 2G3
e-mail: mohamed.chahine@phc.ulaval.ca

and function (Long, Campbell & MacKinnon, 2005a, b; Jiang et al., 2003). The voltage sensor domain of Kv1.2 consists of four transmembrane segments packed together, like the isolated voltage sensor structure of KvAP; but the whole domain is loosely attached to the pore-forming domain and seems almost independent of it. In support of this possibility, novel membrane proteins with a voltage sensor domain and without a pore structure were recently identified (Murata et al., 2005; Sasaki, Takagi & Okamura, 2006; Ramsey et al., 2006).

In the crystal structure of Kv1.2, the S4 segment is adjacent to the S5 segment of the neighboring subunit, placing the S4–S5 linker in an almost antiparallel conformation with the C-terminal end of the S6 segment. It was hypothesized from this observation that S4 has a paddle-like movement materialized by the S3b–S4 region (Jiang et al., 2003). When the ''paddle'' moves, it displaces the S4–S5 linker, which then pushes the S6 segment into a closed conformation, like the position of the homologous segment in the KcsA crystal structure (Long et al., 2005a, b). Another study with the ROSETTA method supported this interaction between the S4–S5 linker and S6 segment but not the paddle movement of S3 and S4 segment (Yarov-Yarovoy, Baker & Catterall, 2006). This study instead suggests a movement of S4 during gating that combines both the helical screw and the transporter models that were previously suggested from experiments (Catterall, 1986; Ahern & Horn, 2004; Chanda et al., 2005). The structures obtained from the crystallographic studies, together with the findings from electron paramagnetic resonance (EPR) spectroscopy experiments (Cuello, Cortes & Perozo, 2004), showed that two S4 arginine residues are exposed to the lipid environment in the open conformation (Long et al., 2005a, b). A more recent study suggested, based on the arginine residues' orientation toward the lipid environment, that the negatively charged phosphodiester groups of membrane lipids are essential to channel function, by neutralizing the S4 segment positively charged residues (Schmidt, Jiang & MacKinnon, 2006). Other studies have shown that these arginine residues are stabilized by forming H-bonds with water molecules from the solvent (Freites et al., 2005; Pradhan, Ghose & Green, 2005; Sands, Grottesi & Sansom, 2005).

The substituted cysteine accessibility approach developed by Karlin & Akabas (1998) was used in the present study. We explored the accessibility of four substituted arginine-to-cysteine residues on the S4 of NaChBac. We also built a homology model of NaChBac based on the crystallographic structures of KvAP and Kv1.2 (Jiang et al., 2002a, b; Long et al., 2005a, b) and used it to characterize how the S4 segment moves in response to changes in membrane potential.

Materials and Methods

Site-Directed Mutagenesis and Recombinant DNA Construction

Recombinant cysteine mutants of the four outermost arginine residues on S4 were generated using QuikChange™ site-directed mutagenesis kits from Stratagene (La Jolla, CA) according to the manufacturer's instructions and as previously described (Chahine et al., 2004). The presence of the mutations was confirmed by automatic sequencing of the entire NaChBac gene (CHUL Research Centre DNA Sequencing Facility, Quebec City, Canada). Wild-type and mutant NaChBac and CD8-a were constructed in the piRES vector (piRES/CD8/NaChBac). For patch-clamp experiments, 2- to 3-day posttransfection cells were incubated for 5 min in medium containing anti-CD8-A-coated beads (Dynabeads M-450 CD8-a, Dynal Biotech ASA, Oslo, Norway) as previously described (Margolskee, McHendry-Rinde & Horn, 1993). Cells expressing surface CD8-a fixed the beads and were visually distinguishable by light microscopy from nontransfected cells (Jurman et al., 1994).

Transfections of the tsA201 Cell Line

tsA201 is a mammalian cell line derived from human embryonic kidney (HEK) 293 cells by stable expression of the SV40 large T antigen (Margolskee et al., 1993). Cells were grown in high-glucose Dulbecco's modified Eagle medium supplemented with fetal bovine serum (10%), L-glutamine (2 mM), penicillin (100 U/ml) and streptomycin (10 mg/ml) (GIBCO BRL Life Technologies, Burlington, Canada). Cells were incubated in a 5% CO_2 humidified atmosphere. tsA201 cell transfections were done using the calcium phosphate method as previously described (Margolskee et al., 1993).

Patch-Clamp Method

Macroscopic Na^+ currents from tsA201-transfected cells were recorded using the whole-cell configuration of the patch-clamp technique (Chahine et al., 2004). Patch electrodes were made from 8161 Corning borosilicate glass and coated with HIPEC R6101, a semiconductor protective coating (Dow-Corning, Midland, MI), to minimize their capacitance. Patch-clamp recordings were made using low-resistance electrodes (≤ 1 MΩ), and a routine series resistance compensation by an Axopatch 200 amplifier (Axon Instruments, Foster City, CA) was performed to values >80% to minimize voltage-clamp errors. Voltage-clamp command pulses were generated by a microcomputer using

pCLAMP software v8.0 (Axon Instruments). Na^+ currents were filtered at 5 kHz, digitized at 10 kHz and stored on a microcomputer equipped with an AD converter (Digidata 1200, Axon Instruments). Data analysis was performed using a combination of pCLAMP software v9.0, Microsoft Excel and SigmaPlot 2001 for Windows v7.0 (SPSS Inc., Chicago, IL).

Solutions and Reagents

For whole-cell recordings, the patch pipette contained 35 mM NaCl, 105 mM CsF, 10 mM ethyleneglycoltetraacetic acid (EGTA) and 10 mM 4-(2-hydroxyethyl)–1-piperazineethanesulfonic acid (HEPES). The pH was adjusted to 7.4 using 1 N CsOH. The bath solution contained 150 mM NaCl, 2 mM KCl, 1.5 mM $CaCl_2$, 1 mM $MgCl_2$, 10 mM glucose and 10 mM Na-HEPES. The pH was adjusted to 7.4 with 1 N NaOH. The liquid junction potential between the patch pipette and the bath solutions was corrected by –7 m*V*. The recordings were made 5 min after obtaining the whole-cell configuration to allow the current to stabilize and the contents of the patch electrode to diffuse adequately. The methanethiosulfonate (MTS) reagents [2-(trimethylammonium) ethyl]-methanethiosulfonate (MTSET), (2-aminoethyl)-methanethiosulfonate (MTSEA) and sodium (2-sulfonatoethyl)-methanethiosulfonate (MTSES) were purchased from Toronto Research Chemicals (North York, Canada). A 2.5-mM stock solution of MTS reagents in water was prepared daily, and aliquots of the stock solution were kept on dry ice until used. To assess closed conformation accessibility, the cells were treated with 500 μM MTS reagent for 5 or 20 min at the cell resting membrane potential to allow the reagent to react with the SH groups of cysteine residues. The MTS reagent was then removed by rinsing, and Na^+ currents were recorded in MTS reagent-free medium. To assess open conformation accessibility, the cells were treated with 500 μM MTS reagent, either in the presence of a high-K^+ solution to depolarize the cells to 0 m*V* or by holding the cells at + 40 m*V* when the *G-V* was shifted beyond 0 m*V*. To study intracellular accessibility, 500 μM MTS reagent was applied via the patch electrode at a holding potential of –140 m*V*. Experiments were carried out at room temperature (22–23°C).

Biophysical Data Analyses

The Na^+ channel conductance (G) was calculated from peak currents (I) according to the equation $G = I/(V - V_{Na})$, where V is the test potential and V_{Na} is the reversal potential determined by the intercept of the linear interpolation of the current before and after reversal. The data points of the *G-V* curve were fitted using the Boltzmann equation, $G/G_{max} = 1/(1 + \exp[(V - V_{½})/k_v])$, where G is the measured conductance, k_v represents the slope factor, $V_{½}$ is the potential at which the half-maximal channel open probability occurs and G_{max} is the maximal conductance.

Homology Modeling

A sequence alignment of NaChBac with KvAP and Kv1.2 was performed using T-Coffee, as in our previous work (Blanchet, Pilote & Chahine, 2007, Notredame, Higgins & Heringa, 2000). According to this sequence alignment, NaChBac has no equivalent residue to the first arginine reside (R1) in other voltage sensor domains. Instead, the first arginine residue (R111) is aligned with R2 in KvAP (R120) and Kv1.2 (R300) and the fourth arginine of NaChBac (R120) is aligned with K5 in Kv1.2. Also, the S3–S4 hairpin is much shorter than that of Kv1.2 and even than that of KvAP. This short length of the voltage sensor of NaChBac had already been reported (Blunck et al., 2004). We used the Kv1.2 crystal structure (2A79 in the Protein Data Bank) to build the pore domain of NaChBac (linker S4–S5, S5 and S6; the selectivity filter was not modeled) (Long et al., 2005a). We used the isolated voltage sensor structure from KvAP (PDB 1ORS) to model the voltage sensor (S1–S4) (Jiang et al., 2003). Homology models of each domain were created using the ZMM program (www.zmmsoft.com) (Zhorov & Bregestovski, 2000; Tikhonov & Zhorov, 2005) by assigning the backbone geometry of the templates to the models. The same assignment was performed for the side-chain geometry of residues conserved in the template and the model.

Energy minimization of the homology model was done using the Monte Carlo (MC) minimization method (Li & Scheraga, 1987) in a multistep relaxation method described elsewhere (Blanchet, Pilote & Chahine, 2007). During MC minimizations, C_α atoms were restrained to 1 Å from their crystallographic coordinates with a flat-bottom energy penalty function. Since the template is considered to be in the open conformation (Jiang et al., 2003; Long et al., 2005b), we used experimental data and the crystal structure of KcsA (Doyle et al., 1998) to model the closed conformation of the pore and manually changed the positions of segments S4 and the S4–S5 linker. Figures of the models were made with PyMol (www.pymol.org).

Statistical Analysis

Data are expressed as means ± standard error of the mean (SEM). When indicated, a *t*-test was performed using statistical software in Sigma Stat for Windows v3.00 (Systat Software, Point Richmond, CA). Differences were deemed significant at $p < 0.05$.

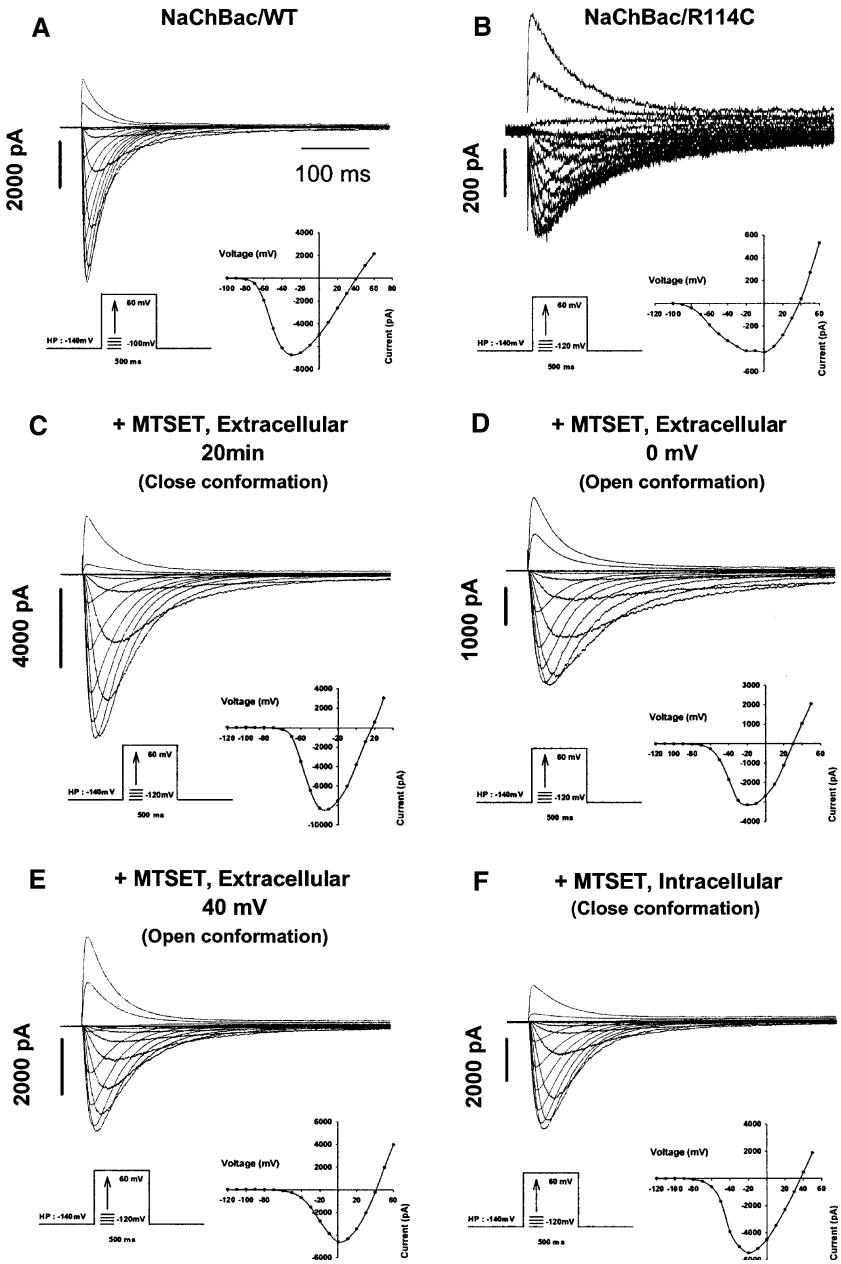

Fig. 1 Family of whole-cell sodium current traces recorded from tsA201 cells expressing (**a**) NaChBac/WT, (**b**) NaChBac/R114C in the presence of MTSET applied from the extracellular space in the closed conformation, (**c**) NaChBac/R114C in the presence of MTSET applied over minutes in the closed conformation, (**d**) NaChBac/R114C in the presence of MTSET applied from the extracellular space in the open conformation (cells treated with high K^+, 0 m*V*), (**e**) NaChBac/R114C in the presence of MTSET applied from the extracellular space in the open conformation (cells clamped at +40 m*V*) and (**f**) NaChBac/R114C in the presence of MTSET applied in the patch electrode in the closed conformation. Currents were generated, from a holding potential of –140 m*V*, from –120 (-100 m*V* for WT) to +50 m*V* for 500 ms in 10-m*V* increments as indicated in the *inset* at the bottom of the figure. The current-voltage relationship (*I-V*), where the maximum Na^+ current was plotted *vs.* the applied voltage corresponding to each current trace, can be seen below each family of current traces

Results

We determined the accessibility of the first four arginine residues of the S4 segment of NaChBac (R111[R1], R114[R2], R117[R3] and R120[R4]) by analyzing the effect on activation (*G-V* curves) of positively and negatively charged MTS reagents (MTSET and MTSES, respectively). MTS reagents were applied in the extracellular solution or in the patch electrode for intracellular accessibility. MTS reagents have no effect on the wild-type NaChBac channel, which is devoid of cysteines, whether applied from the intra- or extracellular space (Chahine et al., 2004). It may therefore be assumed that the effects of MTS reagents observed with mutant channels were related to the presence of the introduced cysteines. Representative current traces of the effects of MTSET on R114C (Fig. 1) and R120C (Fig. 2) illustrate the effect of MTSET on R-to-C mutant channels. The current-voltage relationship (*I-V*), and therefore the *G-V* curves, exhibit shifts (*see below*).

Accessibility of MTSET and MTSES in the Closed Conformation

The accessibility of the substituted arginines of NaChBac was first tested from the extracellular environment in the closed conformation by treating the transfected cells at rest with 500 μM MTSET or MTSES (*see* Materials and Methods). The *G-V* curves of the wild-type (WT) and the

R-to-C mutants before and after MTSET and MTSES treatment are compared in Figure 3 (*see* Table 1 for *G-V* parameters). Note that for the R114C mutant a sum of two Boltzmann functions was required to fit the data; this was also the case in the presence of MTS reagents applied extracellularly or intracellularly (*see below*). As can be seen from Figure 3a, the *G-V* curve of R111C shows a statistically nonsignificant shift in the presence of MTSET, while in the presence of MTSES a significant shift to more depolarized voltages is observed. The R114C mutant channel exhibited a significant shift of the *G-V* curve in the presence of MTSET (Fig. 3b, circles) toward a more hyperpolarized voltage, indicating that the attachment of the positively charged MTS reagent (MTSET) partly restored WT channel activity. This is in agreement with the results obtained in the presence of MTSES (Fig. 3b, squares), where the shift was in the opposite direction, consistent with the presence of a negative charge and with our previous work, where the arginines were substituted with a lysine, a positive charge (Chahine et al., 2004). The *G-V* curves of the R117C (Fig. 3c) and R120C (Fig. 3d) mutant channels were not affected by extracellular application of MTS reagents, suggesting that they were not accessible from the extracellular space.

When MTSET was applied in the patch electrode to explore intracellular accessibility, R120C, R117C and R114C, but not R111C, were affected, as indicated by the shifts in the *G-V* curves (Fig. 4). For unknown reasons, no currents could be recorded when MTSES was applied from the intracellular space for R117C and R120C. It is noteworthy that MTSET shifted the *G-V* curves of R114C and R120C to more hyperpolarized potentials that were intermediate between the WT and the R-to-C mutants. However, when MTSET was applied to the R117C mutant, the *G-V* curve showed a large shift toward depolarized voltages (Fig. 4c). Thus, in the closed conformation, R114C (R2) was accessible from the extra- and intracellular spaces. R117C and R120C were accessible only from the intracellular space, but R111C was not accessible from the intracellular space (*see below for more details*).

Accessibility of MTSET and MTSES in the Open Conformation

To assess the accessibility in the open conformation, tsA201 cells were treated with MTS reagent in the presence of a high K^+ concentration to depolarize them to 0 m*V*. In the case of R114C and R120C and because the furthest shift beyond 0 m*V* of the *G-V* curve occurred when R was replaced by C at these positions, the cells were also treated with MTSET while holding at +40 m*V*. The effects of MTSET on the *G-V* curves for the open conformation are illustrated in Figure 5. As can be seen from Figure 5a, the

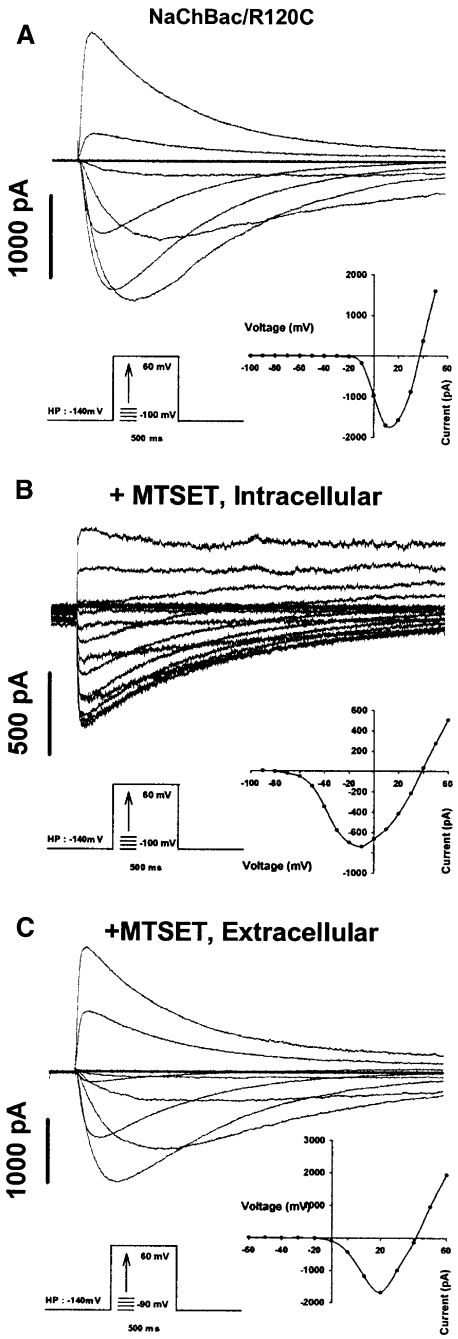

Fig. 2 Family of whole-cell sodium current traces from NaChBac/R120C (**a**) in the presence of MTSET applied in the patch electrode (**b**) and in the presence of MTSET applied from the extracellular space (**c**). Na^+ currents were recorded from tsA201 cells. Currents were generated, from a holding potential of –140 m*V*, from –100 or –80 m*V* to +50 m*V* for 500 ms in 10-m*V* increments as indicated in the *inset* at the bottom of the figure. The current-voltage relationship (*I-V*), where the maximum Na^+ current was plotted *vs.* the applied voltage corresponding to each current trace, can be seen below each family of current traces

G-V curve of R111C shows no shift in the presence of either MTSET or MTSES. However, the effect of MTSET on R114C was evident, with a significant shift of the *G-V*

Table 1 Voltage-dependent activation (*G-V*) parameters

	R111C	R114C	R117C	R120C
Control				
$V_{½}$	–23.27 ± 2.54, n = 12	–27.84 ± 4.18 (0.39) 11.73 ± 2.02 (0.61), n = 15	–32.53 ± 1.35, n = 8	10.93 ± 2.60, n = 8
k_v	–12.83 ± 0.81, n = 12	–15.67 ± 0.58 (0.39) –6.56 ± 0.48 (0.61), n = 15	–10.52 ± 0.70, n = 8	–6.20 ± 0.52 n = 8
MTSET extracellular				
$V_{½}$ (closed)	–23.74 ± 4.35, n = 6	–16.81 ± 3.30,** n = 6	–31.71 ± 2.5, n = 6	14.98 ± 2.37, n = 6
$V_{½}$ (open)	–23.84 ± 2.43,[a] n = 8	–19.26 ± 3.70,[a],** n = 6	–30.09 ± 3.79,† n = 5	10.62 ± 3.18,[a] n = 7
k_v (closed)	–11.99 ± 0.99, n = 6	–9.00 ± 1.01,*,** n = 6	–10.42 ± 0.83, n = 4	–6.66 ± 0.64, n = 5
k_v (open)	–11.01 ± 0.71,[a] n = 8	–12.03 ± 1.35,[a],** n = 6	–9.79 ± 1.00,[a] n = 5	–5.71 ± 0.58,[a] n = 7
MTSET intracellular				
$V_{½}$	–28.11 ± 2.76, n = 5	–28.03 ± 4.28 (0.58) 8.64 ± 6.35 (0.42), n = 5	23.18 ± 2.93,** n = 5	–15.36 ± 5.69,** n = 5
k_v	–12.30 ± 0.31, n = 5	–12.56 ± 1.87 (0.58)* –6.09 ± 2.15 (0.42), n = 5	–6.58 ± 0.88,** n = 5	–13.72 ± 0.60, n = 7
MTSES extracellular				
$V_{½}$ (closed)	–4.18 ± 2.71,** n = 5	–11.89 ± 1.90 (0.50)* 19.29 ± 0.49 (0.50),* n = 7	–30.57 ± 3.83, n = 9	10.49 ± 4.04, n = 5
$V_{½}$ (open)	–17.48 ± 3.64,[a] n = 4	–15.93 ± 0.93(0.49),[a] 18.34 ± 1.01 (0.51), n = 4	n.a.	n.a.
k_v (closed)	–14.68 ± 0.23, n = 5	–15.11 ± 0.65 (0.50) –3.47 ± 1.00 (0.50),** n = 7	–10.93 ± 1.47, n = 9	–6.55 ± 0.78, n = 5
k_v (open)	–13.91 ± 2.19,[a] n = 4	–21.84 ± 2.62 (0.49)[a],** –5.24 ± 0.31 (0.51), n = 4	n.a.	n.a.
+MTSES intracellular				
$V_{½}$	–24.93 ± 2.55, n = 3	–1.45 ± 2.33,*,** n = 4	n.a.	n.a.
k_v	–9.59 ± 1.08, n = 3	–11.89 ± 2.10,*,** n = 4	n.a	n.a.

Values between parentheses are weighing factors; n, number of experiments; n.a., not applicable

* Significantly different from respective control (R to C) parameter ($p < 0.05$), ** $p < 0.01$

[a] In high K^+ extracellular solution

curve to more hyperpolarized voltages (Fig. 5b). R117C and R120C were not accessible, as witnessed by the lack of shift in the *G-V* curves (Fig. 5c,d). Again, as observed in the closed conformation, only R114C is accessible from the extracellular space in the open conformation.

The accessibility of the MTS reagents from inside the cell was not assessed in the open conformation due to technical infeasibility. The low expression of NaChBac in tsA201 cells made it difficult to record Na^+ currents in an excised patch-clamp configuration, which is the most favorable configuration to assess open conformation accessibility from the intracellular space.

Treatment of R111C with MTSEA Reagent

According to previous studies with other channels (Larsson et al., 1996; Yang, George & Horn, 1996; Ahern & Horn, 2005; Ruta, Chen & MacKinnon, 2005), R111C (R1) was expected to be accessible to MTSET from the extracellular space, at least in the open conformation. The absence of a reaction between R111C and MTSET might be due to the bulkiness of this reagent. Indeed, the crystal structure of Kv1.2 as well as EPR studies point to the possibility that R1 may be inserted in the membrane phospholipids (Freites et al., 2005; Long et al., 2005a, b; Cuello et al., 2004). We specifically addressed this issue by treating the cells first with MTSET and then by adding MTSEA in the extracellular solution. If MTSET is able to reach residue R111C but not influence gating, the addition of MTSEA should have no effect. However, the *G-V* curve shift observed (Fig. 6) suggests that even after a 20-min treatment with MTSET, the R111C mutant strongly reacted with MTSEA ($V_{1/2}$ = –55.6 ± 4.5, k_v = 12.47 ± 2.6 m*V* [n = 3] *vs.* $V_{1/2}$ = –28.3 ± 2.7, k_v = 12.3 ± 0.3 m*V* [n = 5]).

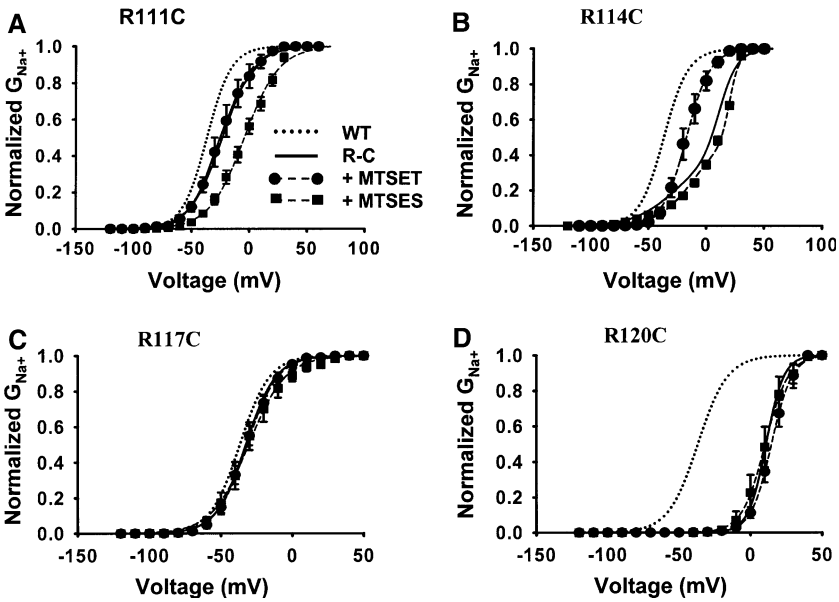

Fig. 3 Voltage dependence of the steady-state activation (*G-V*) of NaChBac/WT and the four R-to-C mutants probed with 500 μM MTSET (*circles*) and MTSES (*squares*) applied from the extracellular space in the closed conformation (**a,** R111C; **b,** R114C; **c,** R117C; **d,** R120C). For the R114C mutant, a sum two Boltzmann functions was required to fit the data. See Table 1 for $V_{1/2}$ and k_v parameters

Therefore, MTSEA-treated channels exhibit a 27-m*V* shift of the $V_{1/2}$ values toward more hyperpolarized potentials without any significant effect on the slope factor, thus supporting the idea that R111C is shielded from MTSET. This effect was coherent with MTSES experiments, which had a significant effect when cells expressing the R111C NaChBac mutant were treated with this reagent (Fig. 3a, squares).

Homology Models of NaChBac

The first homology model built was in the open conformation since the crystal structures of KvAP and Kv1.2 are believed to be in open conformation (Jiang et al., 2003; Long et al., 2005a). A qualitative analysis of this NaChBac model suggests that R111 is shielded from the extracellular milieu by lipids and/or other parts of the proteins. In Figure 7a, the R111 side chain is oriented toward the external side of the voltage sensor and inside the lipid membrane, due to the orientation of the S4 segment (approximately 45° to the membrane). Such orientation of the side chain could make it difficult for fairly large molecules like MTSET to reach R111C. R111 is slightly buried in the lipid membrane, and because of its closeness to the pore and its downward orientation, it is also possible that other residues (L110 in S4, Q165-H166 in S5 and/or W205 in S6) reduce its accessibility to MTSET. The interfacial position (water, lipid and protein) of this residue agrees

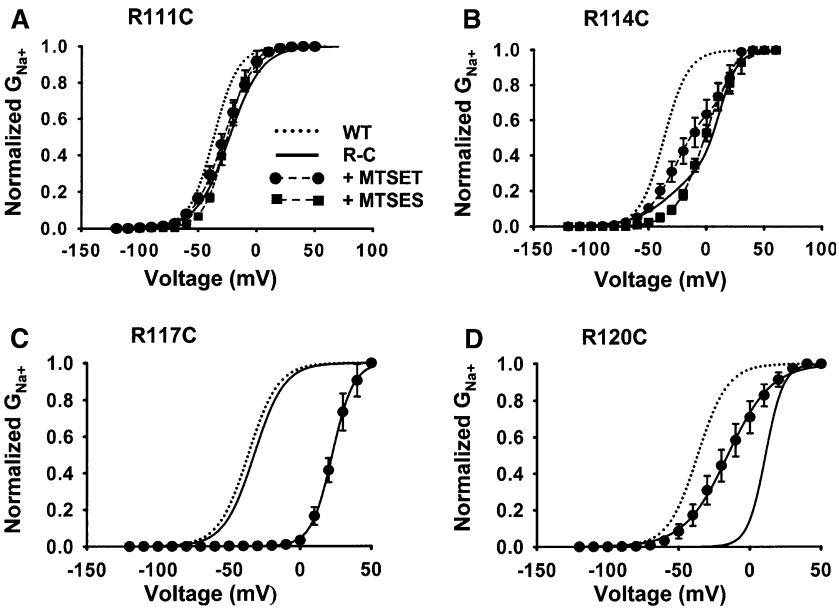

Fig. 4 Voltage dependence of the steady-state activation (*G-V*) of NaChBac/WT and the four R-to-C mutants probed with 500 μM MTSET (*circles*) and MTSES (*squares*) applied from the intracellular space (in the patch electrode) in the closed conformation (**a,** R111C; **b,** R114C; **c,** R117C; **d,** R120C). For the R114C mutant, a sum two Boltzmann functions was required to fit the data. See Table 1 for $V_{1/2}$ and k_v parameters

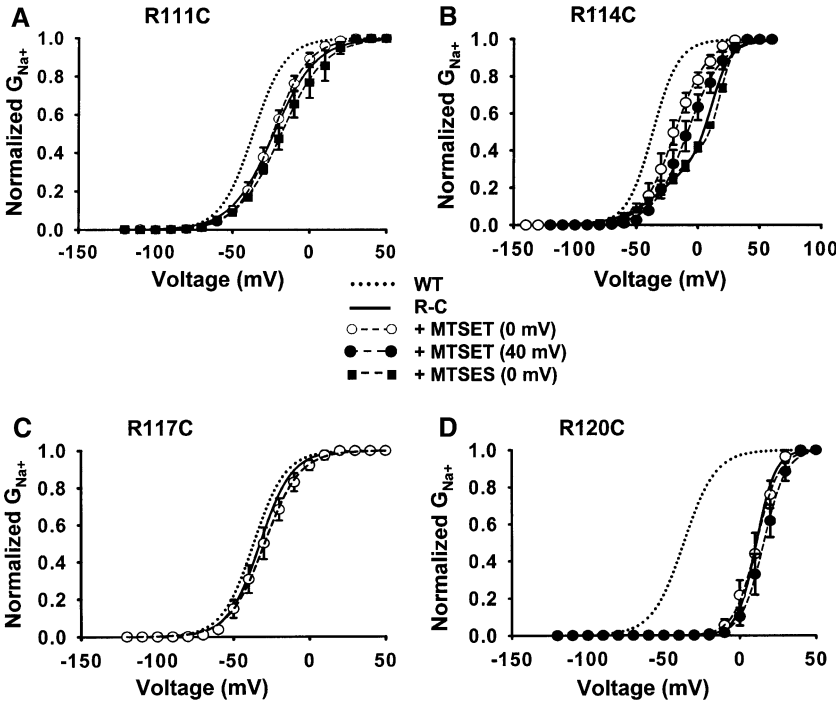

Fig. 5 Voltage dependence of the steady-state activation (*G-V*) of NaChBac/WT and the four R-to-C mutants probed with 500 μM MTSET (*circles*) and MTSES (*squares*) in the open conformation (**a,** R111C; **b,** R114C; **c,** R117C, **d,** R120C). For the R114C mutant, a sum of two Boltzmann functions was required to fit the data. See Table 1 for $V_{1/2}$ and k_v parameters

with an EPR study by Cuello et al. (2004), where R120 in KvAP (R111 in the NaChBac model) is partly protected from the extracellular milieu. R114 and R117 may be readily accessible to MTSET from the extracellular space, while R120 is too deeply buried in the voltage sensor to be accessible (Fig. 7). R117 and R120 were visible through the extracellular crevice, but the crevice might be too small and the residues too deep in the voltage sensor to allow passage of MTSET. The crevice would, however, be large enough to allow the passage of water molecules, which are suggested to stabilize the positive charge of the arginine residues (Sands et al., 2005; Freites et al., 2005). While the accessibility of arginine residues from the intracellular side in the open conformation could not be tested experimentally, the surface representation of the model shows that none of the four arginine residues was visible from this side of the membrane (Fig. 7).

A model of the closed conformation was also built in an attempt to visualize arginine accessibility in this conformation and to simulate the gating movement of S4. To build this model of NaChBac, the S6 segment of the open model was first replaced with an S6 segment constructed from the structure of KcsA (Doyle et al., 1998). The S4–S5 linker was then manually displaced to stay close to S6 in an orientation suggested by Long et al. (2005b). S4 was also manually displaced to remain close to the linker. In the process of moving S4, the segment was tilted, translated and rotated to allow a credible displacement and to respect, as accurately as possible, the experimental data of the closed conformation accessibility.

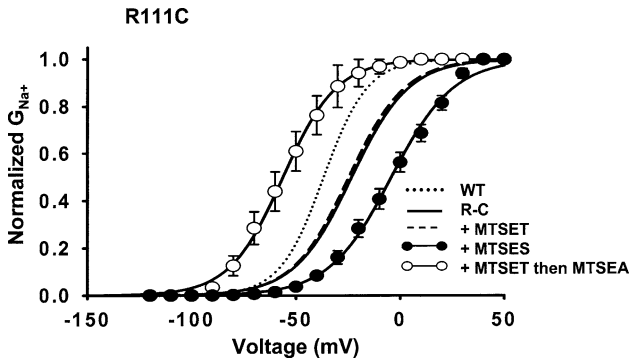

Fig. 6 Voltage dependence of the steady-state activation (*G-V*) of NaChBac/WT (*dotted line*) and the NaChBac/R111C mutant probed with 500 μM MTSET applied extracellularly in the closed conformation for 20 min (*dashed line*), with MTSET then 500 μM MTSEA (*open circles*) or with MTSES (*closed circles*) compared to NaChBac/R111C (*solid line*)

This ''manual modeling'' shows that the transition from the open to the closed conformation of NaChBac only required a small translation of about 2–3 Å across the membrane, a small rotation of 90–100° and a tilt of the helix to allow a peripheral movement of approximately 5–6 Å (Fig. 8). With this movement, R111 and R114 remained visible, explaining the accessibility of R111 to MTSES and of R114 to both MTSET and MTSES. However, R111 was more oriented toward the pore than toward the lipid membrane, and we were unable to make R114 accessible from the intracellular space. R120 appeared to be easily accessible from the intracellular side, and R117, while seemingly accessible, was more deeply buried in the

voltage sensor (Fig. 8). The accessibility of R120C in the model agrees with the experimental data, while that of R117C suggests that attaching a bulky reagent to the residue might hinder the opening movement of S4, requiring a more depolarized potential to provide the necessary electrostatic force to move the S4 segment.

Discussion

In the light of our results, it appears that the accessibility of arginine residues in the S4 segment of NaChBac supports the hypothesis of a small gating movement. Only R114C is accessible to MTSET from the extracellular space, whether the channel is in the open or closed conformation, while R111C is accessible to both MTSEA and MTSES in the closed conformation and not to the bulky reagent MTSET. Homology modeling of the channel showed that R111C might be shielded from MTSET because it is buried at the surface of the lipid membrane or is shielded by other parts of the pore (Long et al., 2005b; Cuello et al., 2004). R114C, R117C and R120C were accessible from the intracellular space in the closed conformation. Experimental data on the open conformation could not be obtained for the intracellular space, but the model of NaChBac indicated that no arginine residues were accessible (Fig. 7c). This is in agreement with the results of Larsson et al., (1996), who reported that R3 and R4 of the *Shaker* K^+ channel are not accessible from the intracellular space in the open conformation. However, we must keep in mind that the surface representations of the models provide only a qualitative explanation.

The results obtained for the accessibility of arginine residues in NaChBac were somewhat different from those for the *Shaker* K^+ and other channels (Larsson et al., 1996; Yang et al., 1996; Bell et al., 2004; Ruta et al., 2005). In *Shaker*, R2 (R111 in NaChBac) is accessible only in the extracellular open conformation and R3 (R114 in

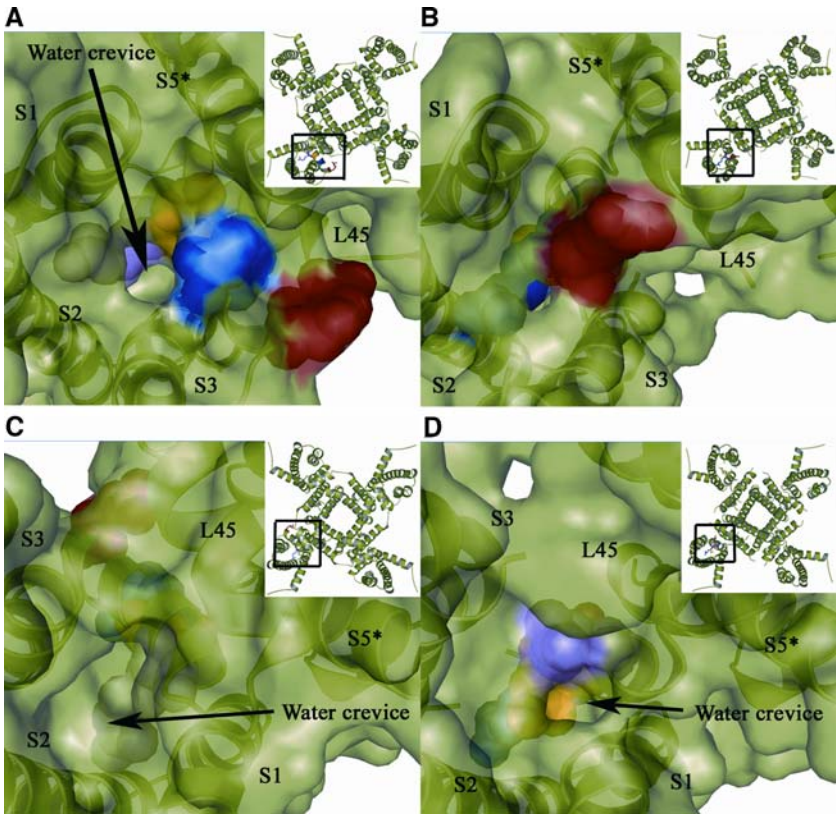

Fig. 7 Surface representation of a NaChBac voltage sensor domain showing arginine residue accessibility. In all panels, R111 is *red*, R114 is *blue*, R117 is *yellow* and R120 is *magenta.* (**a**) Extracellular view of the open conformation, based on KvAP isolated voltage sensor structure, clearly shows that side chains of R111 are partially shielded from the extracellular environment. However, R114 is easily accessible from this side of the membrane. R117 and R120 are also visible through a small hole (the water crevice), but the opening is too small to allow passage of MTS reagent. (**b**) In the extracellular view of the closed conformation, R111 is exposed to the extracellular environment while R114 is not as readily accessible from this side of the membrane. Note the reduction of the water crevice in this conformation. (**c**) Intracellular view of the open conformation only shows a slight part of R120, which does not seem enough to allow access to MTSET. (**d**) Intracellular view of the closed conformation shows that R114, R117 and R120 are visible and might indicate accessibility to MTSET

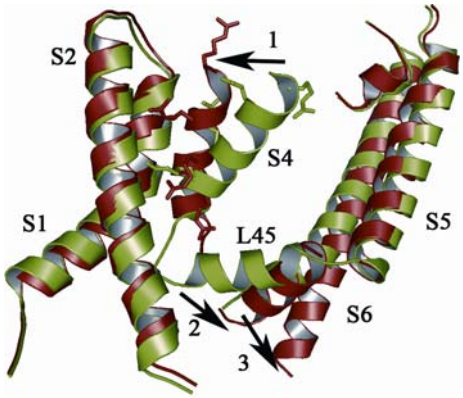

Fig. 8 Conformation change between the open (*green*) and closed (*red*) conformations of NaChBac. The figure shows one subunit in a view parallel to the membrane, with the top being the extracellular side. The S4 segment is rotated by approximately 90° between the open and closed conformations and translated by about 5–6 Å at the periphery of the pore (*arrow 1*). These movements are sufficient to allow a change in R117 and R120 accessibility and to push the S4–S5 linker (L45, *arrow 2*) into the closed confirmation, which in turn pushes S6 (*arrow 3*) into the closed conformation. The C-terminal end of S6 in the open conformation is hidden by the S4–S5 linker in the closed conformation

NaChBac) is only accessible in the intracellular closed conformation. In our study, R111 was not accessible to the bulky reagent MTSET in any conformation, but R114 was accessible to MTS reagents in both conformations from both the intra- and extracellular spaces.

The difference in MTSET accessibility between NaChBac and the *Shaker* K^+ channel may be explained by comparing the amino acid sequences. It appears that NaChBac has a very different arginine pattern compared to other voltage sensors. Sequence alignment with T-Coffee shows the absence of R1. However, when the four arginine residues are aligned (e.g., R111 is R1), NaChBac has no residue homologous to R303 (R5) in Kv1.2 (K374 in *Shaker*) or R133 in KvAP (Blanchet, Pilote & Chahine, 2007). This particular residue has shown important interactions in the *Shaker* K^+ channel (Tiwari-Woodruff et al., 1997; Yarov-Yarovoy et al., 2006). The smaller hairpin conformation of S3–S4 in NaChBac could also create a structural difference in the disposition of the segment or a larger water crevice, allowing easy access to R114 (Larsson et al., 1996). R114 of NaChBac may be situated in the middle of the electric field at the junction between the outer and inner water crevices, as suggested by Sands et al. (2005). Despite a difference in spatial disposition, this could well play a similar role to R1 of the *Shaker* K^+ channel, which has been reported to be involved in the permeation pathway of the cation (Omega) current through the voltage sensor (Tombola, Pathak & Isacoff, 2005). Because we could not assess the accessibility of residues from inside the cell in the open conformation, it is harder to compare the accessibility of R117 and R120 with other channels.

The ''closed conformation'' model was an attempt to understand the movement of S4 between the open and closed conformations, which was not determined by X-ray crystallography. While we were unable to respect all our experimental constraints, our model shows how a relatively small movement of S3b-S4 could generate a conformational change of the pore domain. The peripheral tilt, which has been suggested previously (Elliott et al., 2004; Treptow & Tarek, 2006), thus fits the experimental and modeling data, especially the recent proof of a small movement of S4 (Posson et al., 2005; Chanda et al., 2005; Yarov-Yarovoy et al., 2006), which does not need to be large to differ between the open and closed conformations (Jogini & Roux, 2005; Ruta et al., 2005).

Study Limitations

One limitation of this study is the lack of MTS reagent modification rates. These measurements were not conducted due to the slow gating of the NaChBac channel. The published time constant of MTSET accessibility to potassium channels is on the order of 1 s (Banderali et al., 2004). The slow activation, inactivation and recovery from inactivation (over 5 s) make these measurements difficult.

Conclusion

In this study, we sought to explore the accessibility of arginine residues of the S4 segment of the NaChBac Na^+ channel. In this channel, R111C, the first positively charged residue was not accessible to MTSET in either the open or closed conformation. However, the residue was accessible to smaller reagents (MTSEA and MTSES), suggesting that it might be partially shielded from the bulkier MTSET from the extracellular space through interactions with membrane phospholipids and/or other parts of the channel protein. On the other hand, R114C was accessible to MTSET and MTSES from the extracellular space in both the open and closed conformations. Even more interesting, when the channel was in the closed conformation, R114C was accessible from both sides of the membrane. Base on our model, R114 appeared to be at a junction between the intracellular and extracellular water crevice, a residue conformation that has been previously observed (Tombola et al., 2005; Sands et al., 2005). The accessibility of the arginine residues of NaChBac together with the results of the homology model support the hypothesis of a small movement of the S4 segment for the gating of this channel. However, given that NaChBac is very different from other channels in many ways (shorter

S3–S4 hairpin, fewer positive residues in S4), it is possible that the positions and accessibility of the first four arginines of NaChBac are different from other channels, supporting a recent hypothesis that despite the conserved residues and structural similarity, voltage sensor domains could have different gating movements and intramolecular interactions (Yarov-Yarovoy et al., 2006). Further work with NaChBac, especially the generation of a high-resolution structure, is essential to explain these differences.

Acknowledgement This study was supported by grants from the Heart and Stroke Foundation of Québec and the Canadian Institutes of Health Research. M. C. is an Edwards Senior Investigator (Joseph C. Edwards Foundation). We thank Dr. B. Zhorov for helpful suggestions in developing the NaChBac model and Dr. Dick Horn for suggesting the MTSET/MTSEA experiment on R111C. The authors also thank Sylvie Pilote for excellent technical assistance.

References

Ahern CA, Horn R (2004) Stirring up controversy with a voltage sensor paddle. Trends Neurosci 27:303–307

Ahern CA, Horn R (2005) Focused electric field across the voltage sensor of potassium channels. Neuron 48:25–29

Armstrong CM, Hille B (1998) Voltage-gated ion channels and electrical excitability. Neuron 20:371–380

Banderali U, Klein H, Garneau L, Simoes M, Parent L, Sauve R (2004) New insights on the voltage dependence of the KCa3.1 channel block by internal TBA. J Gen Physiol 124:333–348

Bell DC, Yao H, Saenger RC, Riley JH, Siegelbaum SA (2004) Changes in local S4 environment provide a voltage-sensing mechanism for mammalian hyperpolarization-activated HCN channels. J Gen Physiol 123:5–19

Blanchet J, Pilote S, Chahine M (2007) Acidic Residues on the Voltage-Sensor Domain Determine the Activation of the NaChBac Sodium Channel. Biophys J 92:3513–3523

Blunck R, Starace DM, Correa AM, Bezanilla F (2004) Detecting rearrangements of Shaker and NaChBac in real-time with fluorescence spectroscopy in patch-clamped mammalian cells. Biophys J 86:3966–3980

Catterall WA (1986) Molecular properties of voltage-sensitive sodium channels. Annu Rev Biochem 55:953–985

Chahine M, Pilote S, Pouliot V, Takami H, Sato C (2004) Role of arginine residues on the S4 segment of the *Bacillus halodurans* Na^+ channel in voltage-sensing. J Membr Biol 201:9–24

Chanda B, Asamoah OK, Blunck R, Roux B, Bezanilla F (2005) Gating charge displacement in voltage-gated ion channels involves limited transmembrane movement. Nature 436:852–856

Cuello LG, Cortes DM, Perozo E (2004) Molecular architecture of the KvAP voltage-dependent K^+ channel in a lipid bilayer. Science 306:491–495

Doyle DA, Cabral JM, Pfuetzner RA, Kuo A, Gulbis JM, Cohen SL, Chait BT, MacKinnon R (1998) The structure of the potassium channel: molecular basis of K^+ conduction and selectivity. Science 280:69–77

Elliott DJS, Neale EJ, Aziz Q, Dunham JP, Munsey TS, Hunter M, Sivaprasadarao A (2004) Molecular mechanism of voltage sensor movements in a potassium channel. EMBO J 23:4717–4726

Freites JA, Tobias DJ, von Heijne G, White SH (2005) Interface connections of a transmembrane voltage sensor. Proc Natl Acad Sci USA 102:15059–15064

Hille B (2001) Ion Channels of Excitable Membranes. Sunderland, MA: Sinauer Associates

Jiang Y, Lee A, Chen J, Cadene M, Chait BT, MacKinnon R (2002a) Crystal structure and mechanism of a calcium-gated potassium channel. Nature 417:515–522

Jiang Y, Lee A, Chen J, Cadene M, Chait BT, MacKinnon R (2002b) The open pore conformation of potassium channels. Nature 417:523–526

Jiang Y, Lee A, Chen J, Ruta V, Cadene M, Chait BT, MacKinnon R (2003) X-ray structure of a voltage-dependent K^+ channel. Nature 423:33–41

Jogini V, Roux B (2005) Electrostatics of the intracellular vestibule of K^+ channels. J Mol Biol 354:272–288

Jurman ME, Boland LM, Liu Y, Yellen G (1994) Visual identification of individual transfected cells for electrophysiology using antibody-coated beads. Biotechniques 17:876–881

Karlin A, Akabas MH (1998) Substituted-cysteine accessibility method. Methods Enzymol 293:123–145

Larsson HP, Baker OS, Dhillon DS, Isacoff EY (1996) Transmembrane movement of the shaker K^+ channel S4. Neuron 16:387–397

Li Z, Scheraga HA (1987) Monte Carlo-minimization approach to the multiple-minima problem in protein folding. Proc Natl Acad Sci USA 84:6611–6615

Long SB, Campbell EB, MacKinnon R (2005a) Crystal structure of a mammalian voltage-dependent Shaker family K^+ channel. Science 309:897–903

Long SB, Campbell EB, MacKinnon R (2005b) Voltage sensor of Kv1.2: structural basis of electromechanical coupling. Science 309:903–908

Margolskee RF, McHendry-Rinde B, Horn R (1993) Panning transfected cells for electrophysiological studies. Biotechniques 15:906–911

Murata Y, Iwasaki H, Sasaki M, Inaba K, Okamura Y (2005) Phosphoinositide phosphatase activity coupled to an intrinsic voltage sensor. Nature 435:1239–1243

Notredame C, Higgins DG, Heringa J (2000) T-Coffee: a novel method for fast and accurate multiple sequence alignment. J Mol Biol 302:205–217

Posson DJ, Ge P, Miller C, Bezanilla F, Selvin PR (2005) Small vertical movement of a K^+ channel voltage sensor measured with luminescence energy transfer. Nature 436:848–851

Pradhan P, Ghose R, Green ME (2005) Voltage gating and anions, especially phosphate: a model system. Biochim Biophys Acta 1717:97–103

Ramsey IS, Moran MM, Chong JA, Clapham DE (2006) A voltage-gated proton-selective channel lacking the pore domain. Nature 440:1213–1216

Ren D, Navarro B, Xu H, Yue L, Shi Q, Clapham DE (2001) A prokaryotic voltage-gated sodium channel. Science 294:2372–2375

Ruta V, Chen J, MacKinnon R (2005) Calibrated measurement of gating-charge arginine displacement in the KvAP voltage-dependent K^+ channel. Cell 123:463–475

Sands ZA, Grottesi A, Sansom MS (2005) The intrinsic flexibility of the Kv voltage sensor and its implications for channel gating. Biophys J 90:1598–1606

Sasaki M, Takagi M, Okamura Y (2006) A voltage sensor-domain protein is a voltage-gated proton channel. Science 312:589–592

Schmidt D, Jiang QX, MacKinnon R (2006) Phospholipids and the origin of cationic gating charges in voltage sensors. Nature

Tikhonov DB, Zhorov BS (2005) Modeling P-loops domain of sodium channel: homology with potassium channels and interaction with ligands. Biophys J 88:184–197

Tiwari-Woodruff SK, Schulteis CT, Mock AF, Papazian DM (1997) Electrostatic interactions between transmembrane segments mediate folding of Shaker K^+ channel subunits. Biophys J 72:1489–1500

Tombola F, Pathak MM, Isacoff EY (2005) Voltage-sensing arginines in a potassium channel permeate and occlude cation-selective pores. Neuron 45:379–388

Treptow W, Tarek M (2006) Environment of the gating charges in the Kv1.2 Shaker potassium channel. Biophys J 90:L64–L66

Yang N, George AL Jr, Horn R (1996) Molecular basis of charge movement in voltage-gated sodium channels. Neuron 16:113–122

Yarov-Yarovoy V, Baker D, Catterall WA (2006) Voltage sensor conformations in the open and closed states in ROSETTA structural models of K^+ channels. Proc Natl Acad Sci USA 103:7292–7297

Zhorov BS, Bregestovski PD (2000) Chloride channels of glycine and GABA receptors with blockers: Monte Carlo minimization and structure-activity relationships. Biophys J 78:1786–1803